

## MIXED CHEMISTRY PHENOMENON DURING LATE STAGES OF STELLAR EVOLUTION

R. Szczerba, M.R. Schmidt, M. Pulecka<sup>1</sup>

<sup>1</sup> Nicolaus Copernicus Astronomical Center, ul. Rabiańska 8, 87-100 Toruń,  
Poland

Received 2006 October 15; revised —

**Abstract.** We discuss phenomenon of simultaneous presence of O- and C-based material in surroundings of evolutionary advanced stars. We concentrate on silicate carbon stars and present observations that directly confirm the binary model scenario for them. We discuss also class of C-stars with OH emission detected, to which some [WR] planetary nebulae do belong.

**Key words:** stars: Asymptotic Giant Branch, carbon stars, chemical composition, planetary nebulae, stars: individual (V778 Cyg, IRAS 04496–6859, IRAS 06238+0904, M 2–43)

### 1. INTRODUCTION

During Asymptotic Giant Branch (AGB) phase of evolution stars with initial masses between 0.8 and  $8 M_{\odot}$  lose a significant amount of their initial mass by ejecting the matter into interstellar space with rates between  $10^{-7}$  and  $10^{-4} M_{\odot} \text{ yr}^{-1}$ . The chemistry in the formed circumstellar envelopes is determined by the photospheric C/O ratio and is O-based for  $n(\text{O}) > n(\text{C})$  (usually less evolutionary advanced stars) and C-based when carbon abundance exceeds that of oxygen (evolved stars which experienced thermal pulses and dredged-up carbon to the surface). This dichotomy is a consequence of CO molecule (very stable) formation which is so efficient that less abundant element (C or O) is mostly used. Therefore, the detection of co-existence of O-rich and C-rich material in surroundings of evolved stars was (and still is) surprising and attracts a significant attention. Hereafter, we call this phenomenon a *mixed chemistry phenomenon*.

Already, due to the IRAS observations it was realized that there is a group of carbon stars which show typical for O-rich environment the 9.7 and  $18 \mu\text{m}$  amorphous silicate features (Little-Marenin 1986, Willems & de Jong 1986). The Infrared Space Observatory (ISO) observations (Yamamura et al., 2000) showed that  $9.7 \mu\text{m}$  feature in one of such objects (V778 Cyg) is very stable and did not change during the last 15 years (the time spanned between IRAS and ISO observations). This put a very strong constraint on a model and evolutionary status of this class of objects with most likely explanation being a long-lived reservoir of O-rich material located inside or around a binary system. In this review we discuss MERLIN interferometer observations of V778 Cyg which proved existence of such reservoir (disk) around companion of C-rich star. We note that the recent Spitzer Space Telescope (SST) data showed that the first extra-galactic silicate

carbon star (IRAS 04496–6859, Trams et al. 1999) is in fact a *normal* carbon star and do not show the  $9.7\,\mu\text{m}$  dust emission (see Speck et al. 2006).

There is another group of carbon stars suspected to have mixed chemistry. Namely, carbon stars with OH maser emission. Lewis (1992) listed a group of stars with SiC emission seen in the IRAS Low Resolution Spectra (LRS) and OH maser emission detected. While most of these sources appeared to have wrong LRS classification the 3 C-stars with OH maser emission remained and Chen et al. (2001) added 6 more sources to this class. However, this class of *mixed chemistry* sources did not attract a significant attention (except of [WR] planetary nebulae – see below), since OH emission is not well spatially resolved and this group of sources may be result of spatial coincidence between OH maser emission from interstellar medium and location of C-star. For example, Szczerba et al. (2002) presented observational evidence that IRAS 05373–0810 (C-star with OH maser emission) is a genuine carbon star and that OH maser and SiO thermal emission detected toward this star is not coming from its envelope, but from molecular clouds. Here we discuss a case of another C-star with OH maser emission (IRAS 06238+0904) toward which we have detected, using IRAM radiotelescope, the SiO thermal emission coming from its envelope. Here, we present arguments that shock and Photon Dominated Region (PDR) chemistry allow to form a significant amount of SiO in C-rich environment.

One of the most important achievements of the ISO mission was detection of crystalline silicates. Surprisingly, crystalline silicates were detected also in [WR] planetary nebulae, which have H-poor and C-rich central stars of WR-type<sup>1</sup>. [WR] planetary nebulae show at the same time presence of Polycyclic Aromatic Hydrocarbons (PAHs) and crystalline silicates (Waters et al. 1998, Cohen et al. 1999). Scenarios proposed to explain simultaneous presence of PAHs and crystalline silicates include: destruction of fossil comets orbiting the star, ejection of matter before star become C-rich, formation of stable O-rich disk or torus around companion or system at some point of binary evolution. Hajduk, Szczerba & Gesicki (this Proceedings) present an attempt to determine spatial location of PAHs and crystalline silicates inside the [WR] planetary nebula M 2-43, by means of the radiative transfer modelling of ISO spectrum. They concluded that crystalline silicates have to be located at significant distance from the central star to avoid their emission at about  $10\,\mu\text{m}$ . We note also an attempt to find precursors of [WR] planetary nebulae (C-rich stars with C- and O-rich material in their circumstellar shells) among proto-planetary nebulae (Szczerba et al. 2003). The authors have argued that formation of crystalline silicates is necessary before proto-planetary nebula phase, while post-AGB star may be still O-rich and change to C-rich one during the *fatal* thermal pulse. They indicated five proto-planetary nebulae as a possible precursors of [WR] planetary nebulae, including famous Red Rectangle, other C-rich source with crystalline silicates (IRAS 16279-4757), as well as three O-rich sources which show presence of crystalline silicates in their ISO spectra: AC Her, IRAS 18095+2704 and IRAS 19244+1115.

In this review we will not cover such cases as: NGC 6302 – O-rich planetary nebula which show presence of crystalline silicates as well as PAHs (e.g. Kemper et al. 2002); HD 233517 – an evolved O-rich red giant with orbiting polycyclic

---

<sup>1</sup>Note, that Zijlstra et al. (1991) detected OH maser emission from [WR] planetary nebula IRAS 07027–7934. Therefore, at least this [WR] planetary nebula belongs also to the discussed above class of C-stars with OH maser emission.

aromatic hydrocarbons (Jura et al. 2006); IRAS 09425–6040 – a carbon-rich AGB star with the highest abundance of crystalline silicates detected up to now (Molster et al. 2001); IRC +10216 – a well known C-rich AGB star with water and OH maser lines detected (Melnick et al. 2001, Ford et al. 2003); and possibly some other spectacular sources which we, not intentionally, have overlooked.

## 2. V778 CYG A SILICATE CARBON STAR

To test the hypotheses related to the *mixed chemistry phenomenon* observed in silicate carbon stars, we observed water masers towards V778 Cyg at high angular resolution. Details of our observations and data analysis are presented by Szczerba et al. (2006), so here we repeat only some of the most important points and findings.

The observations were taken on 2001 October 12/13 under good weather conditions, using five telescopes of MERLIN. The longest MERLIN baseline of 217 km gave a fringe spacing of 12 mas at 22.235080 GHz. The bandwidth was 2 MHz with 256 spectral channels per baseline providing a channel separation of  $0.105 \text{ km s}^{-1}$ . The continuum calibrator sources were observed in 16 MHz band with 16 channels. The data were obtained in left and right circular polarisation and the velocities were measured with respect to the local standard of rest.

We used the phase referencing method; 4 min scans on V778 Cyg were interleaved by 2 min scans on the source 2021+614 (at  $3.8^\circ$  from the target) over 11.5 h. The flux density of 2021+614 at K band of 1.48 Jy was derived from observation of 4C39.25. At the epoch of observation the flux density of 3C39.25 was  $7.5 \pm 0.3 \text{ Jy}$  (Teräsraanta 2002, private communication). This source was also used for bandpass calibration.

After initial calibration with the MERLIN software the data were processed using the AIPS package. In order to derive phase and amplitude corrections for atmospheric and instrumental effects the phase reference source was mapped and self-calibrated. These corrections were applied to the target visibility data. The absolute position of the brightest feature at  $-15.1 \text{ km s}^{-1}$  was determined. The phase solutions for this feature were obtained with self-calibration method and were then applied for all channels. The target was mapped and cleaned using a 12 mas circular restoring beam. The map noise of  $\sim 27 \text{ mJy beam}^{-1}$  for  $I$  Stokes parameter in a line-free channel was close to the predicted thermal noise level.

In order to determine the position and the brightness of the maser components two dimensional Gaussian components were fitted to the emission in channel maps. The position uncertainty of this fitting depends on the signal to noise ratio in the channel map and is lower than 1 mas for about 80% of the maser components towards V778 Cyg. The absolute position of the phase reference source is known with an accuracy of  $\sim 3$  mas. The highest uncertainties in the absolute position of maser spots are due to tropospheric effects and errors in the telescope positions. The first effects, estimated by observing the phase rate on the point source 3C39.25, introduce the position error of  $\sim 9$  mas, whereas uncertainties in telescope positions of 1–2 cm cause an error of spot positions of  $\sim 10$  mas. In order to check the position accuracy of maser spots we applied a reverse phase referencing scheme. The emission of 15 channels around the reference feature at  $-15.1 \text{ km s}^{-1}$  was averaged and mapped. The map obtained was used as a model to self-calibrate the raw target data then these target solutions were applied to the raw data of 2021+614.

The position of the reference source was shifted by  $\sim 2$  mas with respect to the catalogue position. This indicates excellent phase connection when referencing 2021+614 to the set of the brightest maser spots. The above discussed factors imply the absolute position accuracy of the maser source to be of order of  $\sim 25$  mas.

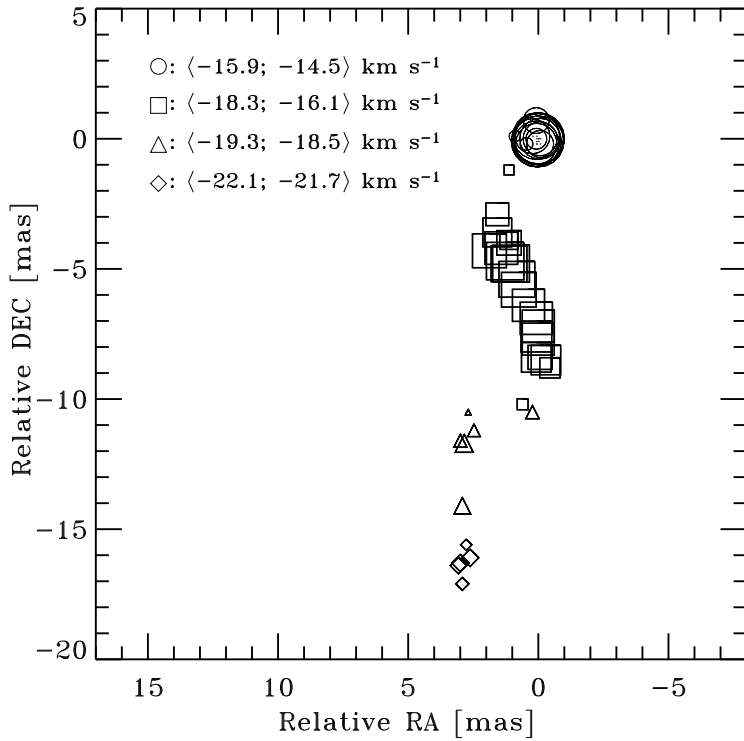


**Fig. 1.** The absolute positions of the  $\text{H}_2\text{O}$  22 GHz maser components towards V778 Cyg relative to the reference feature at  $-15.1 \text{ km s}^{-1}$  ( $\text{RA(J2000)} = 20^{\text{h}} 36^{\text{m}} 07.3833$ ,  $\text{DE(J2000)} = 60^{\circ} 05' 26.024'$ ). The symbols indicate the ranges of component velocities in  $\text{km s}^{-1}$ . The size of each symbol is proportional to the logarithm of peak brightness of the corresponding component.

The maser emission brighter than  $150 \text{ mJ beam}^{-1}$  ( $\sim 5\sigma$ ) was found in 51 spectral channels. In these channels single and unresolved component only was detected. The overall structure of the  $\text{H}_2\text{O}$  maser is shown in Fig. 1. The maser components form a distorted "S" like shape structure along a direction of position angle of about  $-10^\circ$ . There is a clear velocity gradient along this structure with weak south components blueshifted with respect to the brightest north components. The angular extend of maser emission is 18.5 mas. The axis of elongation of the maser structure is fairly perpendicular to the line towards the optical position of V778 Cyg measured by Tycho2 (see Fig. 2). Angular separation between the optical star and the maser reference component is  $0.192 \pm 0.048$ .

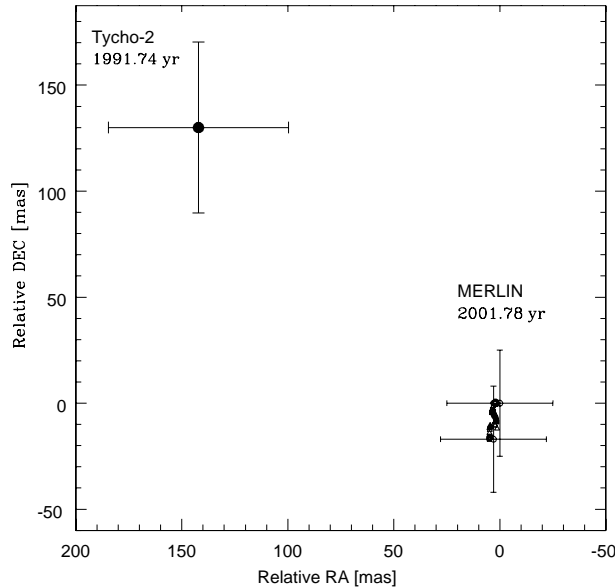


**Fig. 2.** Comparison of the optical position of V778 Cyg as determined in the Tycho-2 catalogue with the radio position of the H<sub>2</sub>O 22 GHz maser components as obtained from the MERLIN measurements. The epochs of optical and radio observations differ by about 10 yrs.

Szczerba et al. (2006) have argued that such separation cannot be explained by proper motion and instead provide direct observational evidence for the binary system model of Yamamura et al. (2000). They suggested that the observed water maser components can be interpreted as an almost edge-on warped Keplerian disk located around a companion object and tilted by no more 20° relative to the orbital plane. More detailed model of disk around companion in V778 Cyg system is presented by Babkovskaja et al. (2006). Finally, note that recently Ohnaka et al. (2006) reported indirect detection of disk around another silicate carbon star (IRAS 08002–38003). They argued that oxygen-rich material is stored in circumbinary disk surrounding the carbon-rich primary star and its putative low-luminosity companion. These two findings may suggest that there are two different kinds of silicate carbon stars: with circumbinary disk and disk around companion only.

### 3. IRAS 06238+0904 - AN OH MASER C-STAR OR GENUINE CARBON STAR?

Genuine carbon stars are formed during evolution on AGB. The star on that stage posses extended circumstellar envelope (CSE). In its inner part (near the photosphere) physical conditions ( $T \sim 2500$  K,  $\rho \sim 10^{14}$  cm<sup>-3</sup>) make the material mainly molecular, with composition determined by the local thermodynamic equilibrium (LTE). In carbon CSE (C/O>1) after CO formation there is almost no oxygen left. However silicon monoxide (SiO) is observed in carbon stars. Recent observations (Schöier et al. 2006) show relatively high SiO fractional abundances ( $1 \times 10^{-7} - 5 \times 10^{-5}$ ), while LTE models give  $\sim 5 \times 10^{-8}$  (Millar 2004). Therefore

the non-equilibrium processes should be considered in modelling of circumstellar chemistry.

In this review we focus on IRAS 06238+0904 – an OH maser C-star (see Chen et al. 2001). We first built model of carbon circumstellar envelope (CSE) and then computed radiative transfer in molecular rotational lines of HCN J=1-0, CS J=3-2, CS J=5-4 and SiO J=3-2, detected by us with the IRAM radiotelescope.

Spectral energy distribution (SED) for IRAS 06238+0904 was modelled by means of the code and method described in Szczerba et al. (1997). The best fit (see Fig. 3) is obtained for the star's effective temperature  $T_*=2500$  [K], luminosity to distance ratio  $L/d^2=6500$  [ $L_\odot \text{kpc}^{-2}$ ], mass loss rate  $\dot{M}=2 \times 10^{-5}$  [ $M_\odot \text{yr}^{-1}$ ], dust temperature at the inner boundary  $T_{\text{dust}}(R_{\text{in}}^{\text{CSE}})=900$  [K], amorphous carbon (AC) and silicon carbide (SiC) to gas ratios:  $\rho(\text{AC})/\rho_{\text{gas}}=0.001$ ,  $\rho(\text{SiC})/\rho_{\text{gas}}=0.00019$ .

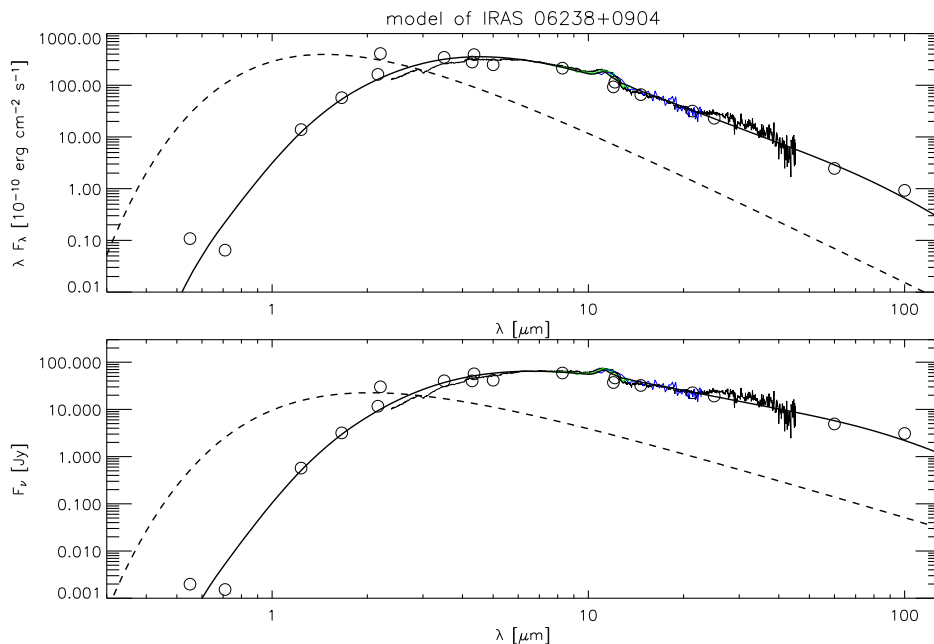


**Fig. 3.** Spectral energy distribution for IRAS 06238+0904. See text for details concerning assumed and estimated parameters.

The chemical model is computed with the network based on RATE99 database Le Teuff et al. (2000) composed of 343 species made of 10 elements. The gas temperature profile is approximated by the power law function  $r^{-1.8}$  established by iterations from the best fits to CS lines. We assume solar gas composition with modifications of carbon ( $\text{C}/\text{O}=1.5$ ) and sulfur  $\epsilon(\text{S})=6.71$  abundances. As initial concentrations we put LTE values of 23 important species, where SiO number density is equal  $1 \times 10^{-8}$  [ $\text{cm}^{-3}$ ] The effect of dust formation is included by reduction of Si and C by amount locked up in SiC and amorphous carbon grains according to dusty model. This results in decrease of silicon abundance to  $\epsilon(\text{Si})=7.39$  and decrease of C to O ratio to 1.3.

The radiative transfer is computed in Sobolev approximation with molecular data taken from the Leiden database (Schöier et al. 2005). Only interstellar radiation is taken into account as an important source of UV photons. Level populations of investigated molecules were computed for the assumed temperature and molecular densities resulting from chemical model. The half-width main beam (HPBW) for SiO rotational transition  $J=3-2$  ( $v=130$  GHz) is equal to  $18.9''$ ,  $16.7''$  for CS(3-2),  $10.0''$  for CS(5-4) and  $28.9''$  for HCN(1-0) transition, in case of the IRAM telescope observations. The synthetic profile was computed for assumed distance to IRAS 06238+0904 being equal 2.3 kpc.

The observed and obtained molecular line profiles of SiO(3-2), CS(3-2) and CS(5-4) are shown in 3 panels of Fig. 4. During line profiles modelling we included simple treatment of CO self-shielding based on Mamon et al. (1988). This process has considerable influence on all molecules, and is especially important for SiO. As one can see in Fig. 4, when self-shielding is not included (solid line) we can explain observed spectrum solely by the PDR chemistry. Around  $1 \times 10^{16}$  [cm] we observed considerable reproduction of SiO. On the other hand, inclusion of CO self-shielding prevents formation of SiO (dashed line). Partial reproduction in PDR is still present. In both cases the exchange reaction  $\text{OH} + \text{Si} \rightarrow \text{SiO} + \text{H}$  is a main process responsible for formation of silicon monoxide. Exchanges between atomic oxygen and SiH, SiC, and HCSi molecules ( $\text{O} + \text{SiH} \rightarrow \text{SiO} + \text{H}$ ,  $\text{O} + \text{HCSi} \rightarrow \text{SiO} + \text{CH}$ , and  $\text{O} + \text{SiC} \rightarrow \text{SiO} + \text{C}$ ) are also important.

Simulation of the shock passage (see Willacy & Cherchneff 1998) enlarge initial abundance of SiO, in comparison to the LTE value, for about one order. Profile obtain with abundance of this molecule increased by factor of 10 is shown as dashed-dotted line in Fig. 4.

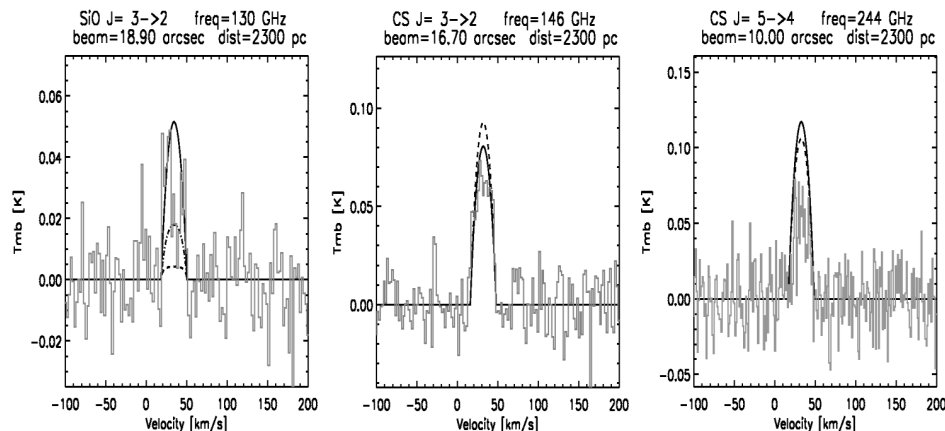


**Fig. 4.** Observed and modelled molecular rotational lines without (solid line) and with (dashed line) CO self-shielding. Dashed-dotted line in the left panel show results when the intial LTE abundance of SiO is increased ten times due to the shock passage.

Therefore, we can conclude that IRAS 06238+0904 is a genuine C-star and no assumption of *mixed chemistry* is necessary. Chemical reactions considered in network can reproduce O-bearing SiO molecule in C-rich environment if no CO self-shielding is considered. In presence of CO self-shielding the computed SiO

emission is too low. This may be improved, however, if we consider the effect of shock passage which can increase the initial SiO abundance by order of magnitude as predicted by Willacy & Cherchneff (1998).

ACKNOWLEDGMENTS. This work has been supported by grants 2.P03D.017.25 and 1.P03D.010.29 of the Polish State Committee for Scientific Research.

## REFERENCES

- Babkovskaia N., Poutanen J., Richards A. M. S., Szczerba R. 2006, MNRAS, 370, 1921  
 Chen P. S., Szczerba R., Kwok S., Volk K. 2001, AA, 368, 1006  
 Cohen M., Barlow M. J., Sylvester R. J. et al. 1999, ApJ, 513, L135  
 Ford K. E. S., Neufeld D. A., Goldsmith P. F., Melnick G. J. 2003, ApJ, 589, 430  
 Jura M., Bohac C. J., Sargent B. et al. 2006, ApJ, 637, L45  
 Lewis B. M., 1992, ApJ, 396, 251  
 Le Teuff Y. H., Millar T. J., Markwick A. J. 2000, A&AS, 146, 157  
 Little-Marenin I. 1986, AA, 307, L15  
 Mamon G. A., Glassgold A. E., Huggins P. J., 1988, ApJ, 328  
 Melnick G. J., Neufeld D. A., Ford K. E. S. et al. 2001, Nature, 412, 160  
 Millar T. J. 2004, in AGB stars, eds. H. J. Habing, H. Olofsson, 247  
 Molster F. J., Yamamura I., Waters L. B. F. M. et al. 2001, AA, 366, 923  
 Ohnaka K., Driebe T., Hoffman K.-H. et al. 2006, AA, 445, 1015  
 Schöier F., Olofsson H., Lundgren A. 2006, AA, 454, 247  
 Schöier F., van der Tak F., van Dishoeck E., Black J. H. 2005, AA, 432, 369  
 Speck A., Cami J., Markwick-Kemper C. et al., 2006, ApJ, 650, 892  
 Szczerba R., Chen P. S., Szymczak M., Omont A. 2002, AA, 381, 491  
 Szczerba R., Omont A., Volk K. et al. 1997, AA, 317, 859  
 Szczerba R., Stasińska G., Siódmiak N., Górný S. K. 2003, in *Exploiting the ISO Data Archive. Infrared Astronomy in the Internet Age*, eds. C. Gry, S. Peschke, J. Matagne, P. Garcia-Lario, R. Lorente, A. Salama, ESA SP-511, 149  
 Szczerba R., Szymczak M., Babkovskaia N. et al. 2006, AA, 452, 561  
 Trams N. R., van Loon J. Th., Zijlstra A. A. et al. 1999, AA, 344, L17  
 Waters L. B. F. M., Beintema D. A., Zijlstra A. A. 1998, AA, 331, L61  
 Willacy K., Cherchneff I., 1998, AA, 330, 676  
 Willems F. J., de Jong T. 1986, ApJ, 309, L39  
 Yamamura I., Dominik C., de Jong T. 2000, AA, 363, 629  
 Zijlstra A. A., Gaylard M. J., Te Lintel Hekkert P. et al. 1991, AA, 243, L9